ELSEVIER

Journal of Chromatography A, 684 (1994) 149–161

JOURNAL OF CHROMATOGRAPHY A

Model of electrophoretic focusing in a natural pH gradient moving in a tapered capillary

Karel Šlais

Institute of Analytical Chemistry, Academy of Sciences of the Czech Republic, 611 42 Brno, Czech Republic

First received 17 May 1994; revised manuscript received 14 June 1994

Abstract

The principle and theoretical description of zone focusing in electrophoretic migration in a tapered capillary are presented. The model involves moving zones which gradually reduce their volume. The variance of a single Gaussian zone is discussed to illustrate the dynamics of this process. In order to derive the solution of the continuity equation, previous models of idealized focusing of ampholytes were modified to represent zone electrophoretic focusing in migration in a capillary with a shallow taper. The relations between the departure from the local steady state, the ratio of the inlet to outlet capillary cross-section, the ampholyte effective mobility and the pH gradient were established. They allow a comparison of described process with conventional isoelectric focusing and also the selection of the operating conditions such that the departure from the local steady state can be decreased to an acceptable extent. The relations predict that focusing in the capillary with a shallow taper should maintain constant the ratio of the actual zone width to the local steady state width, provided that the local capillary cross-section is indirectly proportional to the migration length coordinate. The significance of some assumptions needed for the model formulation is analysed. Numerical examples demonstrate the feasibility of the method.

1. Introduction

The trace determination of ionizable compounds often needs some means of sample concentration. Focusing electrophoretic methods as isotachophoresis (ITP) and isoelectric focusing (IEF) advantageously combine the powerful focusing and separation features. ITP also permits the transfer of analytes from a large capillary cross-section to a smaller one [1–3] which is used also in the combination of ITP with capillary zone electrophoresis (CZE) [4–7]. It has been shown [8] that some modes of IEF, including IEF with electrophoretic mobilization [9–11], have certain features similar to ITP. Therefore, it seems reasonable to examine the possibilities of focusing ampholytes in a capillary with a non-constant cross-section. However, it is known from ITP that migration through a tapered channel brings about deterioration of the boundaries and zone broadening, which needs to be improved by using a coupled capillary with a constant cross-section [3]. Svensson [12] mentioned the idea of the numerical solution of focusing in a channel with a non-constant cross-section.

This contribution presents a simplified theoretical model that allows the shape and the degree of the continuous capillary taper to be related to other operational parameters of the focusing

0021-9673/94/$07.00
SSDI 0021-9673(94)00570-Y

process. The model used is consistent with the simplified approaches used previously to develop the theory of IEF in a channel with a constant cross-section [8,12–16].

2. Description of model

Let us examine focusing with net electrophoretic transport in a capillary with a non-constant cross-section A (see Fig. 1). The initial configuration consists of the near steady-state zone surrounded by the background of volume V_g, which spans the pH gradient with a total pH difference δ(pH). The background together with the ampholytic analyte is positioned between the leading and terminating electrolytes, which adjust the mean gradient effective mobility, $\bar{\mu}$, and, together with the amount of the background components, the pH gradient volume. At time $t = t_0$, the zone position is $y = y_0$, where the capillary cross-section is A_0. Owing to the constant electric current, I, the whole gradient including the analyte zone moves toward the detection point with coordinate y_d and cross-section $A_d < A_0$. Together with the movement to positions with a smaller cross-section, the length of the pH gradient gradually increases. In this way, the local steepness of the pH gradient, d(pH)/dy, decreases and the field strength, E, around the zone increases with decrease in A. The changes in the concentration profile due to the migration into the narrower cross-section unbalance the establishment of the steady state. The ampholyte tends to respond by re-establishing a new steady state but even as this proceeds, the unbalancing effect of the taper continues. With ongoing transport into locations with a smaller cross-section, the steady state remains just out of reach.

To allow the approximate solution of the process described above, the previous simple models of IEF [8,12–16] were used here for the initial considerations. They include the displacement of the gradient components due only to the electrophoretic transport so that the local velocity can be regarded as uniform over the capillary cross-section. Thus, the radial components of the transport can be neglected in comparison with the transport of the zone along the axis of the capillary. The current models of the background in idealized IEF consist of the system of ampholytes with equal diffusion coefficients, D, equal mass of the components and similar derivative of the pH dependence of their effective mobility, dμ/d(pH) around their iso-

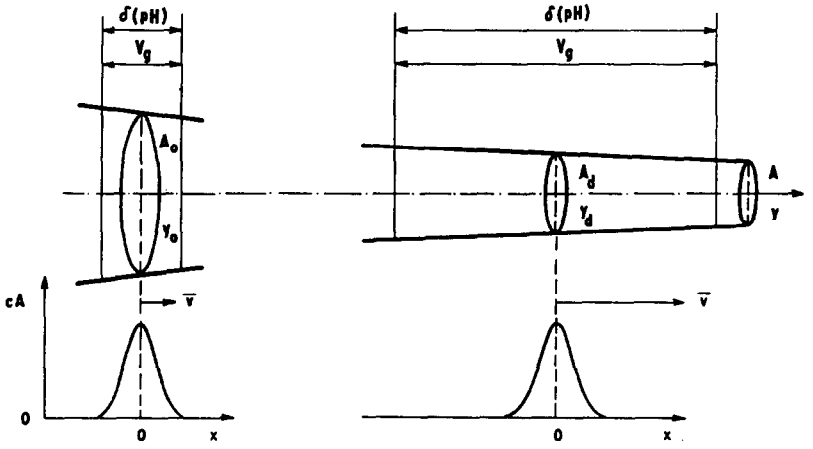

Fig. 1. Model of electrophoretic focusing of ampholytes in a natural pH gradient moving in a tapered capillary. A = Variable capillary cross-section; A_0, A_d = cross-sections at the inlet and at the detection point, respectively; y = separation coordinate, zone position along the capillary axis; y_0, y_d = zone positions at the inlet and at the detection point, respectively; x = distance from the zone centre in the direction of zone migration; c = ampholyte analytical concentration; δ(pH) = pH difference across the volume of the separation medium, V_g; $\bar{v}$ = zone mean velocity along the separation coordinate. For further explanation, see text.

electric point, pI. The analyte amount is assumed to be small enough to make no essential contribution to the properties of the background. Because of the large number (up to thousands) of background components with approximately equally spaced isoelectric points, an essentially linear gradient is formed in the capillary of constant cross-section. The large number of components and a sufficiently large field strength imply that the zone width is small in comparison with the length of the capillary. Further, the contribution of solvent ions to the background conductivity is neglected. Assumptions of constant steepness of the pH gradient and constant field strength around the zone in a capillary with constant cross-section used previously in order to develop a theory simple enough for practical use do not, in fact, imply any serious oversimplification [14].

The above models are modified here in such a way that the pH gradient and the peak of the ampholytic analyte are allowed to move electrophoretically in the capillary with a shallow taper. The electric current, I, is constant, which implies a constant volume displacement of the considered zone. The pH difference, δ(pH), over the volume of the focusing medium, V_g, and its conductivity are regarded as independent of the field intensity. Further, the ampholyte net dissociation is allowed to be small so that the local pH is not very different from the component isoelectric point, pI, which enables the derivative of the component mobility vs. pH dependence, $\mathrm{d}\mu/\mathrm{d}(\mathrm{pH})$, to be regarded as equal to that at its pI. The mean effective mobilities of the components of the background and also that of the analyte are determined by the $\mathrm{d}\mu/\mathrm{d}(\mathrm{pH})$ parameter and the composition of the leading electrolyte. As the diffusivities of both the background components and analyte are here considered to be the same, their mean effective mobilities can still be regarded as mutually equal. Hence it is accepted that the field intensity varies along the capillary due only to the current density. As the above conditions are not very different from the steady state in IEF, it is reasonable to regard the concentration profile of the zone as a Gaussian curve [8,12–18].

3. Theory

3.1. Relation of zone variance to the gradient of migration velocity

In the initial part of the theory, let us describe the influence of the local migration velocity, v, on the zone width as outlined in the model description and Fig. 1. The zone is regarded as that of the analyte or that of the background component. As the local velocity can be regarded as uniform over the capillary cross-section and the zone is close to the steady state, the radial concentration gradients can be neglected in comparison with the axial ones. When we accept the above assumptions, the continuity equation for the considered ampholyte can be written in a one-dimensional form:

$$\frac{\mathrm{d}c}{\mathrm{d}t} = D \cdot \frac{\mathrm{d}^2c}{\mathrm{d}y^2} - \frac{\mathrm{d}(vc)}{\mathrm{d}y} \tag{1}$$

where c is the local concentration of the ampholyte. The transformation to the system in which the coordinate origin moves with the zone centre enables the concentration changes to be related to the position of the concentration maximum. In the new system, x is the distance from the zone centre, expressed as

$$x = y - \int_0^t \bar{v}\,\mathrm{d}t \tag{2}$$

where $\bar{v}$ is the mean zone velocity along the separation coordinate, $\bar{v} = \mathrm{d}y/\mathrm{d}t$. Actually, it is the local velocity of the zone concentration maximum. With the use of Eq. 2, Eq. 1 transforms to

$$\frac{\mathrm{d}c}{\mathrm{d}t} = D \cdot \frac{\mathrm{d}^2c}{\mathrm{d}x^2} - c \cdot \frac{\mathrm{d}v}{\mathrm{d}x} - (v - \bar{v}) \cdot \frac{\mathrm{d}c}{\mathrm{d}x} \tag{3}$$

As stated above, electrophoretic focusing with transport in the tapered capillary leads to non-steady-state zones. This means that the term $\mathrm{d}c/\mathrm{d}t$ in Eq. 3 is different from zero. Whereas in a capillary with constant cross-section the local steady-state concentration profile remains constant along the capillary axis [8], the local steady-state concentration profile in a tapered capillary

changes owing to the variations in the field strength and pH gradient. If the actual profile approaches the local steady-state profile very rapidly, it could be described by the relationships used in the description of the simple model of IEF. As the flux that equilibrates the difference between the actual profile and local steady state is only finite, the actual profile only tends to reach the local steady-state profile. Hence, the zone dispersion varies both by changes in the local steady-state profile and by the departure of the actual profile from the steady-state profile. As the concentration profile is regarded as Gaussian, the temporal changes in the local concentration originated by both effects can be expressed with help of the apparent dispersion coefficient, D^*, by the relation

$$\frac{dc}{dt} = \frac{d}{dx} \cdot \left(D^* \cdot \frac{dc}{dx} \right) \tag{4}$$

The insertion of Eq. 4 into Eq. 3 yields

$$\frac{d}{dx}\left[(D - D^*) \cdot \frac{dc}{dx} \right] = c \cdot \frac{dv}{dx} + (v - \bar{v}) \cdot \frac{dc}{dx} \tag{5}$$

In a tapered capillary, the local actual velocity, v, varies with the local cross-section, A, and thus with the x coordinate. As a shallow taper is considered, this variation can be described by a Taylor expansion. However, the shape of the capillary taper may be generally very different. In order to permit a simplified analytical solution of Eq. 5, we shall examine only a single kind of taper which generates a velocity variation described by only the first two terms in the expansion

$$v = \bar{v} + x \cdot \frac{dv}{dx} \tag{6}$$

By insertion of Eq. 6 into Eq. 5 and coupling the exact differential, we obtain

$$\frac{d}{dx}\left[(D - D^*) \cdot \frac{dc}{dx} \right] = \frac{dv}{dx} \cdot \frac{d(cx)}{dx} \tag{7}$$

As long as the dv/dx term is treated as a constant in the entire capillary, Eq. 7 can be directly integrated. The assumption of a long capillary in comparison with the zone width means that the boundary conditions imply vanishing of the concentration and the appropriate derivations towards both capillary ends. We obtain after integration, the use of the relation $dc/(c\,dx) = d(\ln c)/dx$ and rearrangement,

$$(D - D^*) \cdot \frac{d(\ln c)}{dx} = x \cdot \frac{dv}{dx} \tag{8}$$

The Gaussian concentration profile can be described by the relation

$$c = c_{max} \exp\left(\frac{-x^2}{2\sigma^2} \right) \tag{9}$$

where σ is the standard deviation of the curve in length units and c_{max} is the concentration in the zone concentration maximum, where $x = 0$. Since, as will be verified further, σ can be regarded as a constant along the whole capillary, from Eq. 9 it is for the particular zone

$$\frac{d(\ln c)}{dx} = \frac{-x}{\sigma^2} \tag{10}$$

By insertion of Eq. 10 into Eq. 8, we obtain the sought relation between the length-based zone variance and the constant velocity gradient. For further treatment, it is convenient to write this relation in the form

$$\frac{D^* - D}{\sigma^2} = \frac{dv}{dx} \tag{11}$$

Below, dv/dx and D^* will be expressed in terms of mobility, field strength and capillary taper.

3.2. Gradient of migration velocity in a tapered capillary

As the zone is transported only by the electromigration, the component velocity is the product of the component effective mobility, μ, and the local field strength, E:

$$v = \mu E \tag{12}$$

The focusing occurs by means of two gradients in the direction of the transport, the mobility gradient and field strength [12,15,18]. As the curvature of the velocity gradient is shallow, the same is expected for the both of the above. Further, the zone width is regarded as small in comparison with the capillary length. These gradients

can then be approximated as linear within the zone. The actual effective mobility can then be related to the mobility gradient, $d\mu/dx$, within the zone by the relation

$$\mu = \bar{\mu} + x \cdot \frac{d\mu}{dx} \quad (13)$$

Let us remember again that $\bar{\mu}$ is the component effective mobility at the zone maximum (see also Fig. 2). The mobility gradient of the ampholyte, $d\mu/dx$, can be related to the background pH gradient, d(pH)/dx, by the equation

$$\frac{d\mu}{dx} = \frac{d\mu}{d(pH)} \cdot \frac{d(pH)}{dx} \quad (14)$$

where $d\mu/d(pH)$ is the gradient of the pH dependence of the component effective mobility. It is generally function of μ but, as the ampholyte $\bar{\mu}$ is here constant and the zones are narrow, the $d\mu/d(pH)$ term can be regarded as constant within the zone. This approximation is similar to that made in the simple IEF models with the only difference that the mean effective mobility of the zone centre is different from zero. As stated in the model description, the background pH gradient can be treated as the pH continuum. In the steady state, it generates a linear pH gradient in a capillary of constant cross-section. The influence of variable capillary cross-section on the local steepness of the pH gradient can be expressed as

$$\frac{d(pH)}{dx} = A \cdot \frac{\delta(pH)}{V_g} \quad (15)$$

where δ(pH) is the pH difference over the gradient volume, V_g. As the ratio $\delta(pH)/V_g$ is constant, it allows us to assume that the local pH gradient can be expressed by Eq. 15 also when the background composed of a series of zones of ampholytes moves in the capillary with a non-constant cross-section under conditions that are close to the steady state. It should be noted that V_g can be only a fraction of the capillary volume and only a small part of that volume which surrounds the particular zone can be taken into the consideration for the estimation of the local steepness of the pH gradient. Therefore, the volume-based steepness of the pH gradient need not be constant over the whole V_g. When this is the case, then, instead of $\delta(pH)/V_g$, the volume steepness of the pH gradient can be written in terms of the small finite differences, $\Delta(pH)/\Delta V_g$.

The local field strength is related to A by the equation

$$E = \frac{I}{\kappa A} \quad (16)$$

where I is the total electric current over the capillary cross-section and κ is the background electrolyte conductivity. In conventional IEF, the background conductivity is inversely proportional to the degree of separation of the background component or, in other words, to the field intensity. However, in IEF with electrophoretic mobilization, this influence is reduced owing to the presence of a common counter ion which adjusts the non-zero mean effective mobility of both the background and the analytes. In Section 4, the conditions will be specified under which the background conductivity can be regarded as constant. Similarly to

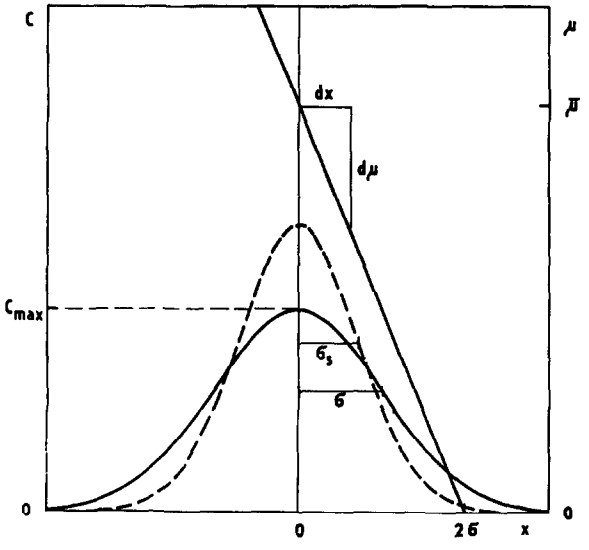

Fig. 2. Illustration of the zone mobility and the zone width. σ, σ_s = Actual and local steady-state standard deviation of the zone concentration profile, respectively; c_{max} = maximum ampholyte concentration in the zone; $d\mu/dx$ = derivative of the dependence of the ampholyte effective mobility on the distance along the separation coordinate; $\bar{\mu}$ = the zone mean effective mobility. For further explanation, see text.

the description of the local pH gradient, the conductivity need not be constant over the entire V_g. It is sufficient when the κ of the background surrounding the considered zone is constant. Therefore, in subsequent considerations, a constant conductivity environment of the particular zone during its transport through the tapered capillary is taken as a first approximation. When the constant current is applied to a tapered capillary filled with a medium of the constant conductivity, we obtain for the derivative of the dependence of the field strength on x with use of Eq. 16

$$\frac{dE}{dx} = -E \cdot \frac{d \ln A}{dx} \tag{17}$$

For evaluation of the dv/dx term in Eq. 11, the product $E\, d\mu/dx$ has an important role. The combination of Eqs. 14, 15 and 16 gives

$$E \cdot \frac{d\mu}{dx} = \frac{d\mu}{d(pH)} \cdot \frac{\delta(pH)}{V_g} \cdot \frac{I}{\kappa} \tag{18}$$

It appears that, for the first approximation, the $E\, d\mu/dx$ term can be regarded as independent of the capillary cross-section; the increase in E by the capillary taper is just counterbalanced by the same decrease in the $d\mu/dx$ term. It further yields the invariability of the $E\, d\mu/dx$ term with respect to the position relative to the zone centre not only in a capillary with a constant cross-section but also in a tapered capillary. This conclusion has key importance in the treatment of zone variance in the next section. Further, when we take the $E\, d\mu/dx$ term as constant, it can be verified with the use of Eqs. 12, 13 and 17 that the sought relation for the velocity gradient, dv/dx, is

$$\frac{dv}{dx} = E \cdot \frac{d\mu}{dx} - E\,\bar{\mu} \cdot \frac{d(\ln A)}{dx} \tag{19}$$

Insertion of Eq. 19 in Eq. 11 yields the relation

$$\frac{D^* - D}{\sigma^2} = E \cdot \frac{d\mu}{dx} - E\bar{\mu} \cdot \frac{d(\ln A)}{dx} \tag{20}$$

which brings us closer to the final solution.

3.3. Departure from the local steady state

Now, let us consider the system with no mean electrophoretic transport of the zone, i.e., $\bar{\mu} = 0$. It corresponds to the simple model of IEF, which means $dc/dt = 0$ and $D^* = 0$ in the steady state. Applying this condition to Eq. 20 yields the known relation for the length-based variance of the focused Gaussian zone in the steady state, σ_s^2 [8,12–16]:

$$\sigma_s^2 = \frac{-D}{E \cdot \frac{d\mu}{dx}} \tag{21}$$

Together with conclusion following from Eq. 18, the last relation indicates that, under the approximations made, the length-based width of the steady-state focused zone is independent on the capillary cross-section. Further, as $dx = dy$ for the steady state (see Eq. 2), σ_s is constant along the entire capillary. This conclusion also supports the assumptions used for the derivation of Eqs. 10 and 11. However, the steady-state volume-based standard deviation expressed as $A\sigma_s$ decreases proportionally to the decrease in A. As the model adopted involves the background composed from the series of ampholyte zones with the same amounts of respective components, c_{max} is proportionally higher for the zones positioned at the smaller cross-section relative to the zones focused at larger A.

Now, let the series of the zones move from the broader end of the capillary towards the narrower end. When this movement is very slow, the zones can almost adjust their concentration profiles to the local steady-state ones. The result of such a process would be a continuous increase in c_{max} of every particular zone. According to the model adopted, the position with certain A is bound to the corresponding c_{max} for every zone passed. However, when we are treating a particular moving zone, the assumption of equal amounts of the gradient components is not necessary. Therefore, we can follow a single moving zone of an analyte in the same way as the zone of the background.

As discussed in Section 3.1, the zones moving

in a tapered capillary do not reach the local steady-state profile. When comparing Eq. 21 with Eq. 20, we can see that there are two terms more in the relation for the focusing with the finite mean zone velocity, i.e., D^*/σ^2 and $\bar{\mu}E\,\mathrm{d}(\ln A)/\mathrm{d}x$, which make the difference from the description of the local steady state. The departure from the equation for the steady-state focusing arises from the fact that the transport of the zone through a tapered capillary prevents a steady state from occurring.

First, the higher field strength in front of the zone continuously speeds up this part of the zone relative to the centre. Similarly, the zone rear, where the field strength is smaller relative to the centre, is slowed. This source of departure relative to the steady state is described by the second term on the right-hand side (RHS) of Eq. 20.

Second, as σ_s is constant and we examine a system with a small departure of the actual σ from σ_s, the ever decreasing capillary cross-section sweeps the concentration in the zone maximum to an increase relative to the actual value. As the zone concentration profile remains Gaussian, this process seems like negative diffusion towards the zone centre. This contribution to the departure of the actual state from the steady state reflects the term D^*/σ^2 in Eq. 20.

Owing to this effect, the steady state remains just out of reach, with the actual zone width lagging slightly behind the local steady-state zone width. The diagram of concentration profiles in Fig. 2 illustrates the above description; the standard deviation of the actual concentration profile exceeds the local steady state one.

Further, we shall discuss here the case when the actual zone width can be expressed as a multiple of the local steady state width with a proportionality coefficient not very different from unity. This is advantageous when the departure from the steady state is small and finite over the entire capillary. Then the proportionality coefficient should also be constant. To conclude, we shall seek a shape of the capillary taper that should maintain the ratio of the actual to the local steady-state zone width constant and not very different from unity.

It is conventional to express the changes in zone dispersion in terms of plate height, H. Then, we may relate D^* to H and the zone mean velocity explicitly as

$$D^* = \frac{\bar{v}H}{2} \tag{22}$$

Although the use of the theoretical plate concepts is particularly inappropriate for continuous processes, the rate of variance generation, $H = \mathrm{d}\sigma^2/\mathrm{d}y$, is still of utmost significance. It applies also for techniques operating in a non-uniform, gradient mode [17–19]. Thus, more universally, H may be regarded as a local increment of the zone variance. For a capillary with a non-constant cross-section, the volume-based changes in zone variance, σ_v^2, should apply. As a shallow taper is under consideration, the theoretical plate volume can be expressed as the product of H and A. Then, we can write for H

$$H = \frac{1}{A} \cdot \frac{\mathrm{d}\sigma_v^2}{\mathrm{d}V} \tag{23}$$

and for σ_v, $\sigma_v = \sigma A$. The length-based zone variance may be regarded here as constant, to a first approximation (see also Eqs. 18 and 21). Then, the volume-based changes of the zone variance are originated from the variation of the cross-section along the separation coordinate. As $\mathrm{d}V = A\,\mathrm{d}y = A\,\mathrm{d}x$, we obtain from Eq. 23

$$H = 2\sigma^2 \cdot \frac{\mathrm{d}(\ln A)}{\mathrm{d}x} \tag{24}$$

It should be noted that, contrary to the common understanding, there is some difference in the meaning of H. In conventional kinetic processes, e.g., in chromatography, the local departure from equilibrium leads to an increase in the zone variance. Here, the causality is changed, i.e., the continuously forced change in the volume-based variance leads to the departure from its local steady-state value.

Further, following Eq. 12, the local mean zone velocity is

$$\bar{v} = \bar{\mu}E_0 \tag{25}$$

where E_0 is the field intensity at the zone centre.

For a narrow zone in a capillary with a shallow taper, E and E_0 can be related by

$$E = E_0 + x \cdot \frac{dE}{dx} \tag{26}$$

E_0 in Eq. 25 may be approximated by E when the second term on the RHS of Eq. 26 is much smaller than the first, $|x\,dE/dx| \ll |E_0|$. When applied to a zone with width 4σ, this condition can be written with help of Eq. 17 as

$$2\sigma \ll \frac{-1}{d(\ln A)/dx} \tag{27}$$

In Section 4, the conditions for the use of E instead of E_0 will be further specified. With the last approximation, the insertion of Eqs. 24 and 25 in Eq. 22 yields the sought relation for D^*:

$$D^* = \bar{\mu} E \sigma^2 \cdot \frac{d(\ln A)}{dx} \tag{28}$$

Finally, insertion of Eq. 28 into Eq. 20 yields the expression for the actual zone variance:

$$\sigma^2 = \frac{D}{E\left[2\bar{\mu} \cdot \frac{d(\ln A)}{dx} - \frac{d\mu}{dx}\right]} \tag{29}$$

The last equation is more general than Eq. 21 because both for the zero net mobility and/or for no taper, it converts to the equation for σ_s. However, it should be kept in mind that Eq. 29 is derived for conditions where the denominator of the RHS is treated as constant or, in other words, for a special kind of capillary taper. Nevertheless, the last equation shows that the focused zone can be obtained, provided that the first term in the brackets is smaller than the second and, for a small departure of the actual zone width from the local steady-state one, it should be even much smaller. For a more explicit formulation of this relation, let us introduce the departure from the local steady state, ϵ, by the equation

$$\epsilon = 1 - \frac{\sigma_s^2}{\sigma^2} \tag{30}$$

This term not only simplifies the subsequent equations, but also explicitly relates the actual zone variance to the local steady-state one. Apparently, the smaller ϵ is, the closer is the zone to the local steady state; zero ϵ means achieving the local steady state. The magnitude of ϵ can obtained by the treatment of the equations for σ^2 and σ_s^2. From combination of Eqs. 21, 29 and 30, we arrive at the relation between the capillary taper, the effective mobility gradient and ϵ as a simple expression achieving the desired purpose:

$$\frac{d(\ln A)}{dx} = \frac{\epsilon}{2} \cdot \frac{d\mu/dx}{\bar{\mu}} \tag{31}$$

By insertion of Eqs. 14 and 15 into Eq. 31, we obtain for the steepness of the capillary taper explicitly

$$\frac{d(1/A)}{dx} = \frac{\epsilon}{2} \cdot \frac{-d\mu/d(\mathrm{pH})}{\bar{\mu}} \cdot \frac{\delta(\mathrm{pH})}{V_g} \tag{32}$$

A relation similar to Eq. 32 can be obtained by evaluation of the changes in the resolution of the zones focused with migration in a tapered capillary [20]. The last equation can be used to calculate the relation of the capillary geometry to the acceptable departure from the steady state as a function of other experimental parameters.

3.4. Relation between the capillary geometry and the departure from the local steady state

Eq. 32 relates the local capillary taper to ϵ and important parameters of focusing such as the gradient volume and pH difference, the analyte mobility and the mobility vs. pH dependence. For the evaluation of the feasibility of the method, the dependence of the departure from the steady state on the entire capillary geometry is necessary. The following calculations are formulated so that the geometrical parameters are expressed as explicit functions of other experimental parameters including ϵ, which is regarded as a constant determined by the acceptable departure of the actual zone profile from the local steady-state one (see Eq. 30).

Because, for the sought geometry, the whole RHS of Eq. 32 and the zone volume displacement are regarded as positive constants along the

entire length of the capillary, the x variable can be substituted back to the y coordinate. After integration, we have for the dependence of the local cross-section on the y coordinate

$$A = \frac{1}{y} \cdot \frac{2}{\epsilon} \cdot \frac{\bar{\mu}}{-\mathrm{d}\mu/\mathrm{d(pH)}} \cdot \frac{V_g}{\delta(\mathrm{pH})} \tag{33}$$

When we solve the equation obtained for the particular capillary dimensions, let us recall that the cross-section A_0 is at the beginning of the capillary, $y = y_0$, and the cross-section A_d is at the detection point, $y = y_d$ (see Fig. 1). Then, the capillary length is $L = y_d - y_0$. Further, it is convenient to relate the changes in the capillary cross-section to its narrowest value, A_d. Therefore, we introduce the ratio of the inlet cross-section to the detection cross-section as a ratio, q:

$$q = A_0/A_d \tag{34}$$

Then, the particular solution of Eq. 32 has the form

$$1 - \frac{1}{q} = \frac{\epsilon}{2} \cdot \frac{-\mathrm{d}\mu/\mathrm{d(pH)}}{\bar{\mu}} \cdot \frac{\delta(\mathrm{pH})}{V_g} \cdot A_d L \tag{35}$$

The parameter q is also related to the capillary volume, V_L, which can be obtained by integration:

$$V_L = \int_{y_0}^{y_d} A \, \mathrm{d}y \tag{36}$$

By insertion of Eqs. 33 and 34 into Eq. 36, we obtain after integration

$$\ln q = \frac{\epsilon}{2} \cdot \frac{-\mathrm{d}\mu/\mathrm{d(pH)}}{\bar{\mu}} \cdot \frac{V_L}{V_g} \cdot \delta(\mathrm{pH}) \tag{37}$$

Usually, capillaries of circular cross-section are used with $A = \pi r^2$, where r is the local capillary radius. With help of Eqs. 33 and 37, the sought dependence of r on y can be formulated as a relation involving only the geometrical parameters:

$$r = \left(\frac{1}{y} \cdot \frac{V_L}{\pi \ln q} \right)^{1/2} \tag{38}$$

which indicates the decrease in the capillary radius with the square root of the y coordinate. The needed V_L and q variables should be optimized with the help of the previous equations.

4. Discussion

For the discussion of the calculation procedure, Eq. 32 has a key position. It relates the capillary taper to the departure from the steady state, ϵ, steepness of the pH gradient, $\delta(\mathrm{pH})/V_g$, and the relative change in compound mobility vs. pH. Note that no electrical variables enter this equation except for their influence on the assumption of a narrow zone. As postulated in course of the calculation, the departure from the steady state which can be expressed in terms of ϵ is set constant along the whole capillary. The second term in Eq. 32 is the property of the focused substance and the magnitude of its effective mobility adjusted by the leading electrolyte. Therefore, it is independent of the capillary shape. The volume-based steepness of the pH gradient can be considered as constant for small departures from the steady state. Hence the left-hand side (LHS) of Eq. 32 can be regarded as a constant which determines the capillary geometry described by Eqs. 33–38. On the other hand, the invariability of the LHS of Eq. 32 justifies some approximations made through the calculations. Namely, together with Eq. 16, it leads to invariability of the $\mathrm{d}E/\mathrm{d}x$ term in Eq. 17, which further justifies Eq. 26 and leads to invariability of the $\mathrm{d}v/\mathrm{d}x$ term expressed by Eq. 19. Finally, for the found capillary shape, it also means that no higher terms need be neglected when writing the relation for the actual v (Eq. 6).

The assumption of constant conductivity has been used throughout this theory to facilitate and simplify the calculations. Now, the significance of this assumption will be discussed in a semi-quantitative manner. In the model adopted, the changes in average effective mobility of the ampholyte within the zone have contributions from changes in the ratios of uncharged and positively and negatively charged forms of the particular ampholyte with mutual overlap of the neighbouring zones. According to the model

adopted, the separation of the zone maxima in volume units is regarded as independent of field strength and capillary cross-section. Hence the mutual overlap is determined by the zone width in volume units. When there is no counter ion, the relative content of both ionized forms of the ampholyte decreases in the same way as the zone volume becomes smaller. When some strong common counter ion (e.g., positive) is used, the state can be achieved when the fraction of one of the charged forms of the ampholyte (i.e., positive) decreases faster than the other and finely becomes negligibly small. With further zone sharpening, the fraction of the other dissociated form (i.e., negative) remains constant in order to maintain the finite mean mobility that is necessary for transport of the whole gradient. To conclude, the relative invariability of the conductivity of the zone environment with the field intensity can be achieved when most of the respective ampholyte of the background is ionized with charge of only one sign. Then, its effective charge cannot vary with the zone width and then it also cannot be function of field, and, under a constant total current, a function of cross-section and position along the capillary length. As most of the component is accumulated within the zone width expressed as 4σ (see Fig. 2), such a condition can be described by the relation

$$2\sigma < \frac{-\bar{\mu}}{\mathrm{d}\mu/\mathrm{d}x} \tag{39}$$

This relation shows that under the conditions prescribed, a change in the sign of the ampholyte effective charge occurs at a point that is more than 2σ distant from the zone centre and hence only a negligible fraction of the total ampholyte mass has a charge sign opposite to that of most of the component. It is apparent that in IEF where zero net mobility is adjusted, the background conductivity is always dependent on the zone shape. On the other hand, in focusing with electrophoretic mobilization where the common counter ion adjusts the finite net effective mobility, it is possible to achieve a certain σ where the conductivity remains constant with further decrease in σ. Now, as the zones are close to the steady state, let us estimate the desired conditions from the combination of Eqs. 14, 21 and 39. In the case of migration of the gradient towards the cathode, we obtain for E

$$E > \frac{4D}{\bar{\mu}} \cdot \frac{-\mathrm{d}\mu/\mathrm{d(pH)}}{\bar{\mu}} \cdot \frac{\mathrm{d(pH)}}{\mathrm{d}x} \tag{40}$$

Let us examine the real conditions close to the detection point as the reference and the narrowest, most critical place. We take typical values for focusing of ampholytes with electrophoretic mobilization towards the cathode as the ampholyte mean effective charge $z = 0.1$ and $E = 50$ V mm^{-1} [8]. With the use of the Nernst equation, we can estimate the first term on the RHS of Eq. 40 as $4\,RT/zF \approx 1$ V. The second term does not exceed 10 pH^{-1} for biprotic ampholytes and $z \approx 0.1$. As the gradient volume is usually only a fraction of the capillary volume in methods with gradient mobilization, let us take $V_g = V_L/5$. Further, we take $V_L/A_d = 200$ mm, which relates the discussed tapered capillary to the typical length of a capillary with constant cross-section. The typical pH difference across the pH gradient is taken as $\delta(\mathrm{pH}) = 5$ pH. Then, Eq. 15 gives 0.125 pH mm^{-1} for the third term of the RHS of Eq. 40. Together, this means that E should be >1.25 V mm^{-1} at $y = y_d$. Actually, E can be expected to be up to 50 V mm^{-1} at the detection point [8], which is nearly two orders of magnitude higher than Eq. 40 needs. Consequently, with the help of Eqs. 33 and 34, the conductivity should not vary considerably with changes in A even at q up to about 50 in the discussed case. It can be noted that when the background components can be treated as weak electrolytes with similar D and equally spaced pK_a values [8], the conductivity of the background should not vary with the shape of the zone of its components.

The zone profile at the focusing in a pH gradient in a background with a linear conductivity gradient was calculated by Svensson [12] for $\bar{\mu} = 0$ and $\mathrm{d}E/\mathrm{d}x = 0$. Under these conditions, he found the equation for the skew concentration distribution. When, for a shallow conductivity gradient, his result (Eq. 34 in Ref.

[12]) is taken and the logarithm is expanded as $\ln(1+a) = a + a^2/2 - a^3/3$ with neglect of higher terms, we obtain in the present notation

$$\ln\left(\frac{c}{c_{max}}\right) = \frac{-x^2}{2\sigma_s^2}\left[1 + \frac{2}{3}\left(1 - \frac{\kappa}{\kappa_0}\right)\right] \quad (41)$$

where κ_0 is the conductivity at the zone centre. As the change in conductivity within a narrow zone can be expected to be only a few per cent, the actual concentration profile can be still approximated by a Gaussian curve.

Further, with decrease in A, the field strength increases and the conductivity can be constant or can decrease when the zone approaches the narrow parts of the capillary. At constant I, a field strength increase higher than corresponds to the decrease in A can be expected when the assumption of constant conductivity is not appropriate. Hence, although the calculations may become complicated with variation of the conductivity, narrower zones than those predicted by Eqs. 21 and 29 can be expected.

From Eqs. 27 and 31, the condition for approximating E_0 by E is

$$\frac{1}{\sigma} \gg \epsilon \cdot \frac{-\mathrm{d}\mu/\mathrm{d}x}{\bar{\mu}} \quad (42)$$

which is surely met when the system obeys Eqs. 39 and 40 as ϵ is expected to be much smaller than unity.

As the amount of the ampholyte in the zone and the length-based zone width remain constant during migration in a tapered capillary, the product of the local concentration and the local cross-section should have the same profile independent of the zone position in the capillary (see Fig. 1, bottom). Hence, as the zone passes through the tapered capillary, the concentration in the zone maximum increases proportionally to the decrease in cross-section (see also discussion following Eq. 21). Explicitly, the ratio of the inlet to the outlet concentration in the zone maximum is expected to be equal to q.

The acceptable numerical value of q may be estimated from the semi-quantitative evaluation of Eq. 37. For ampholytic analytes such as proteins, the absolute value of the second term on the RHS is 10 pH^{-1} or higher for $z = 0.1$. When we take values of V_g and δ(pH) the same as those for the evaluation of E at the detection point, it appears that the ratio q may be up to hundreds even for accepted ϵ as small as $0.01 < \epsilon < 0.1$.

The example of capillary dimensions with $V_L/A_d = 200$ mm and $q = 10$ can be calculated as follows. The combination of Eqs. 35 and 37 yields the length of the tapered capillary, $L = V_L(1 - 1/q)(A_d \ln q) = 78$ mm, which is a factor of 0.39 smaller than the length of a cylindrical capillary of the same V_L and A_d. When we take the values above, we obtain $\epsilon = 0.0184$ from Eq. 37. With help of Eq. 30, this leads to the conclusion that the actual σ can be expected to be only 1% higher than the local steady state σ_s in the discussed case. It is apparent that a higher acceptable ϵ permits a higher q (see Eq. 37). For example, departure from the steady state due to the capillary taper expressed as $\epsilon = 0.5$ may be practically acceptable because, according to Eq. 30, it represents a σ/σ_s ratio of 1.4 (see Fig. 2). It can be concluded that there need not be a substantial decrease in the separation efficiency in comparison with other possible sources of the departure of the actual zone width from the theoretical local steady state value expressed by Eq. 21.

The course of the ratio of the local capillary radius to the radius at the detection point, r_d, with the position along the capillary is shown for q values of 5, 10 and 20 in Fig. 3. For the calculation of the curves, Eq. 38 is modified to

$$\frac{r}{r_d} = \left[\frac{1}{\frac{(y - y_0)A_d \ln q}{V_L} + \frac{1}{q}}\right]^{1/2} \quad (43)$$

where the V_L/A_d ratio is taken as constant and equal to 200 mm. In viewing Fig. 3, it should be kept in mind that the curves are drawn with $L/r_d \approx 5$, whereas in reality the values of this ratio can be expected to be up to two orders of magnitude higher. For example with $q = 20$ and typical $r_d = 40$ μm, $L/r_d \approx 1600$. Thus, even the shape with $q = 20$ can still be regarded as a shallow taper along the entire capillary.

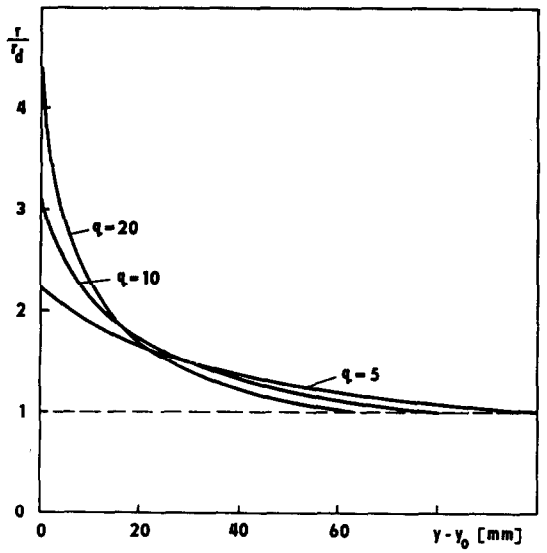

Fig. 3. Examples of calculated capillary geometry for $V_L/A_d = 200$ mm. r/r_d = Ratio of local capillary radius to the radius at the detection point; $y - y_0$ = distance from the capillary inlet; q = ratio of inlet capillary cross-section to the cross-section at the detection point.

Eqs. 32, 33 and 37 clearly show that the increase in the allowable taper steepness and/or the decrease in ϵ can be achieved by a decrease in the zone mean effective mobility. Thus, the smaller $\bar{\mu}$ is, the steeper the decrease in the capillary cross-section (or the higher q) can be with the same other parameters including ϵ. As follows from the model description, the mean effective mobility of an ampholytic analyte and that of the background components can be conveniently controlled by the leading electrolyte composition.

5. Conclusions

A simplified model of the focusing of an ampholyte zone that migrates electrophoretically in a tapered capillary has been suggested. An approximate solution of the continuity equation is possible by assuming a constant conductivity environment of the zone during its electrophoretic transport within a capillary with a shallow taper. It was found that focusing in the tapered capillary should maintain constant the departure of the actual zone width from the local steady-state zone width and acceptably small even for a considerable ratio of the inlet to outlet capillary cross-section, provided that the local capillary cross-section is indirectly proportional to the migration length coordinate. The equations derived enable one to show the magnitude of the possible gain in operational parameters such as the decrease in the voltage and pressure drop needed, which will be discussed elsewhere together with changes in the zone resolution [20].

The method described opens up the way to increase the number of separable compounds without limitation from the excessive high voltage needed. The intended use of a constant current may obviate the problems of record interpretation associated with operation under a constant potential drop.

The discussed non-steady-state process continuously transports, separates and focuses the Gaussian zones of the ampholytes or of weak electrolytes, so it can be seen as intermediate between typical electrophoretic techniques including CZE, ITP and IEF.

6. References

[1] F.M. Everaerts, T.P.E.M. Verheggen and F.E.P. Mikkers, *J. Chromatogr.*, 169 (1979) 21.
[2] T.P.E.M. Verheggen and F.M. Everaerts, *J. Chromatogr.*, 249 (1982) 221.
[3] V. Dolník, M. Deml and P. Boček, *J. Chromatogr.*, 320 (1985) 89.
[4] F. Foret, V. Šustáček and P. Boček, *J. Microcol. Sep.*, 2 (1990) 229.
[5] F. Foret, E. Szökö and B. Karger, *J. Chromatogr.*, 608 (1992) 3.
[6] D.S. Stegehuis, H. Irth, U.R. Tjaden and J. van der Greef, *J. Chromatogr.*, 538 (1991) 393.
[7] D.S. Stegehuis, U.R. Tjaden and J. van der Greef, *J. Chromatogr.*, 591 (1992) 341.
[8] K. Šlais, *J. Microcol. Sep.*, 5 (1993) 469.
[9] S. Hjertén and M. Zhu, *J. Chromatogr.*, 346 (1985) 265.
[10] S. Hjertén, J. Liao and K. Yao, *J. Chromatogr.*, 387 (1987) 127.
[11] S. Hjertén, K. Elenbring, F. Kilár, J.L. Liao, A.J.C. Chen, C.J. Siebert and M.D. Zhu, *J. Chromatogr.*, 403 (1987) 47.
[12] H. Svensson, *Acta Chem. Scand.*, 15 (1961) 325.

[13] M. Almgren, *Chem. Scr.*, 1 (1971) 69.
[14] H. Rilbe, *Ann. New York Acad. Sci.*, 209 (1973) 11.
[15] J.C. Giddings and H. Dahlgren, *Sep. Sci. Technol.*, 6 (1971) 345.
[16] J.C. Giddings, *Sep. Sci. Technol.*, 14 (1979) 871.
[17] J.C. Giddings, *Dynamics of Chromatography, Part I*, Marcel Dekker, New York, 1963.
[18] J.C. Giddings, *Unified Separation Science*, Wiley, New York, 1991.
[19] J.C. Giddings, *Anal. Chem.*, 35 (1963) 353.
[20] K. Šlais, *J. Microcol. Sep.*, submitted for publication.